A LOW-LOSS 1.8GHZ MONOLITHIC THIN-FILM PIEZOELECTRIC-ON-SUBSTRATE FILTER

Wanling Pan, Reza Abdolvand, and Farrokh Ayazi*
School of ECE, Georgia Institute of Technology, Atlanta, GA, USA
(* Now with the School of ECE, Oklahoma State University, OK, USA)

ABSTRACT

A 1.8GHz thin-film piezoelectric-on-substrate (TPoS) filter with insertion loss of less than 4dB and bandwidth of 18MHz (50Ω termination) is presented in this paper. Such filters are alternatives to conventional ladder-type filters working in the frequency range of up to a few GHz. A monolithic TPoS filter is a coupled mode system based on a single composite resonant structure, with a thin piezoelectric layer deposited on a high acoustic velocity, low loss substrate layer. An interdigitated top electrode structure is used that eliminates the spurious modes and provides a mechanism for adjusting the bandwidth.

1. INTRODUCTION

Thin film bulk acoustic resonators (FBARs) are widely used in modern communication systems [1, 2]. To achieve the desired passband width and out-of-band rejection, multiple FBARs are usually electrically connected to build a ladder-type filter, resulting a filter size in the order of $1\times1mm^2$[2]. Alternatively, acoustically coupled resonator filters [3, 4] have been investigated to offer an integrated solution with better out-of-band rejection by eliminating the large feedthrough capacitor intrinsic in the ladder-type filters.

In this work, we report on the development of the thin-film piezoelectric-on-substrate (TPoS) filters, which are micromachined version of the conventional monolithic crystal filters. In previous work [5], the reported insertion loss (IL) of TPoS filters was more than 10dB in the GHz regime, much higher than the commercial FBAR filters in the same frequency range. To fully explore the potential of the TPoS design, we analyze the various loss mechanisms in a TPoS filter and report on our improved design and fabrication techniques. A TPoS filter with 3.6dB IL at 1.82GHz is demonstrated, proving its competence in communication applications. It is also shown that by designing the layout of the electrodes, bandwidth adjustment is possible for such a filter. From the analysis of the measurements, various factors influencing the IL are investigated, and the proposed optimizations demonstrate TPoS filters' competence in high-performance communication systems.

2. OPERATION PRINCIPLE AND DESIGN

The basic structure of a TPoS filter is shown in Fig. 1(a). The resonant structure consists of a thin piezoelectric film on a low loss substrate layer, such as Si or diamond. Two electroded regions are acoustically coupled in the bulk of this composite structure. The two resonant regions can vibrate in-phase (Fig. 1(b)) or 180° out-of-phase (Fig. 1(c)), creating a coupled mode system with fourth-order transfer function. The stress-free low acoustic loss substrate layer in this structure provides for structural integrity and high Q resonance modes which in turn enables filters with narrow bandwidth.

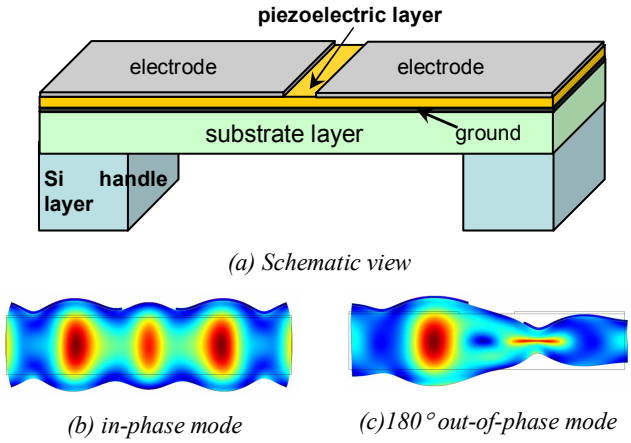

(a) Schematic view

(b) in-phase mode *(c)180° out-of-phase mode*

Figure 1. The schematic view and the resonance mode shapes of a thickness-mode TPoS filter.

Such a filter can be modeled by the equivalent circuit shown in Fig. 2 [6]. The circuit consists of two resonant branches (R_m, L_m, C_m) coupled by an inductor L_c. A capacitor C_f is added to account for the feedthrough between the two ports. An investigation of the equivalent circuit reveals that the high IL of a TPoS filter mainly originates from three factors: high series resistance (R_m), large shunt capacitance (C_p) and small shunt resistance (R_p). The series resistance R_m mainly comes from the mechanical damping transformed to the electrical domain and is directly related to both the mechanical damping factor and the effective electromechanical coupling factor of the structure. The transmission line resistance also contributes to the value of R_m. The value of C_p is mostly determined by the static capacitance of the electroded regions. And the shunt resistance represents loss from the leakage current and

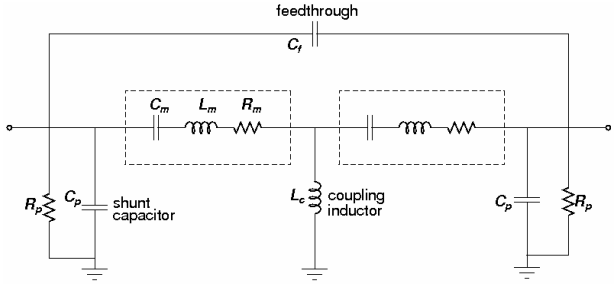

Figure 2. The equivalent circuit of a TPoS filter.

dielectric loss from the material. Thus the improvement of the IL can be realized by improving the quality of the piezoelectric layer, by eliminating the leakage current, by choosing a piezoelectric material of low dielectric damping, and by cancelling the shunt capacitance.

Both the device structure and the fabrication process are designed to address these issues. High-resistivity Si is chosen as the substrate layer, with an additional SiO_2 passivation layer, to reduce transmission loss. A thin SiO_2 layer is deposited between the bottom electrode and the piezoelectric layer. This oxide layer serves as insulation and eliminates the leakage from the top to the bottom electrode. A thick Ag layer of a few microns is added to the transmission line, taking advantage of its high conductivity to reduce the electrical loss.

From our prior work, it was observed that a simple design such as the one in Fig. 1(a) results in excitation of numerous spurious modes which makes the technique ineffective. By implementing an interdigitated (IDT) pattern for the top electrodes, the spurious modes are significantly suppressed. Using IDT top electrodes promotes concentration of acoustic energy in the two specific in-phase and out-of-phase thickness modes and reduces the coupling coefficient for other spurious modes. In Fig. 3, frequency responses of two filters with the simple design and the IDT design are compared. Each sharp peak in the frequency plot of Fig. 3 (a) corresponds to an excited unwanted mode.

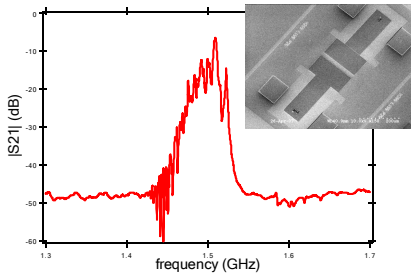

(a)

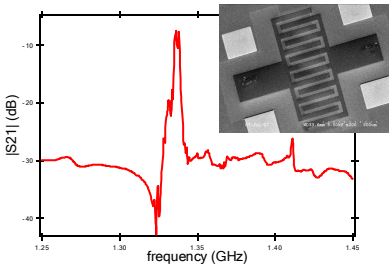

(b)

Figure 3. Typical frequency response of filters with (a) two simple rectangular electrodes and (b) IDT electrodes.

3. FABRICATION AND MEASUREMENTS

TPoS filters are fabricated on an SOI wafer with a high resistivity (>4000Ω·cm) Si device layer of about 2.5µm thickness, as illustrated in Fig. 4. A 1µm-thick SiO_2 passivation layer is deposited on the device layer. This layer is patterned at the filter area to minimize mechanical loading to the resonant structure. A SiO_2 mask layer is deposited and patterned on the backside of the wafer for future etching. A bottom electrode and ground plane metal of Ti/Au of 30/100nm thickness, a 30nm-thick SiO_2 insulating layer, and a ZnO layer of about 1.2µm thickness are deposited subsequently. The ZnO and the SiO_2 layers are then etched to open contact for the ground plane. A top electrode of 100nm-thick Al is defined on top of the ZnO layer. A thick Ag layer of 4µm thickness is deposited and patterned on the signal line and ground plane to minimize transmission line resistance. Finally, the Si handle layer is etched from the backside using the predefined oxide mask, and the buried oxide layer is removed subsequently. The temperature of the process does not exceed 300°C and the process is compatible with the standard CMOS process. The SEM image of a filter is shown in Fig. 4(f).

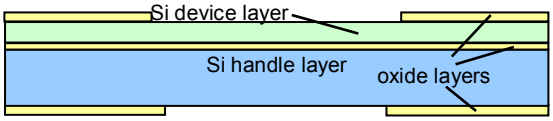

(a) Oxide layer deposition and patterning

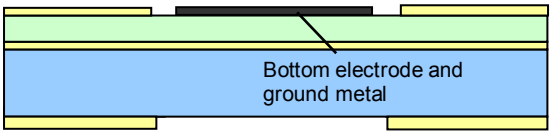

(b) Bottom electrode deposition and patterning

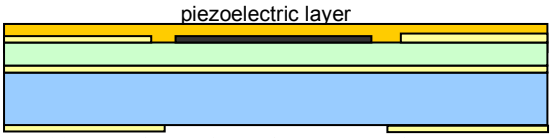

(c) Piezoelectric layer deposition and patterning

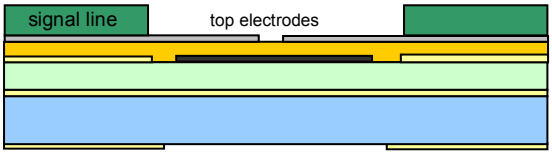

(d) Top electrode and signal line patterning

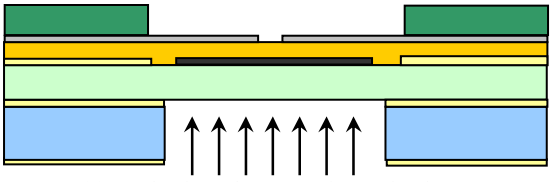

(e) Backside etching to release the device

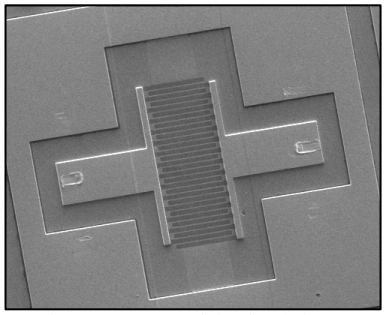

(f) SEM image of the final device

Figure 4. The abbreviated process flow of the TPoS filter.

TPoS filters are measured in an Agilent E8364B network analyzer with GSG type probes and 50Ω termination. The $|S_{21}|$ and $|S_{11}|$ plots of a filter are shown in Fig. 5, where the resonance peak of the second thickness mode is at 1.82GHz and is in good agreement with the prediction from Mason's model [7, 8]. The filter has an IL of 3.6dB and a bandwidth of 18MHz. This performance is comparable to commercial ladder-type FBAR filters, such as those used in GPS applications [1]. The top electrodes have an IDT structure with 10 pairs of 10μm-wide fingers separated by 3μm. The bottom electrode is 100μm wide, making the active filter area as small as 100μm×260μm, significantly more compact than ladder-type FBAR filters.

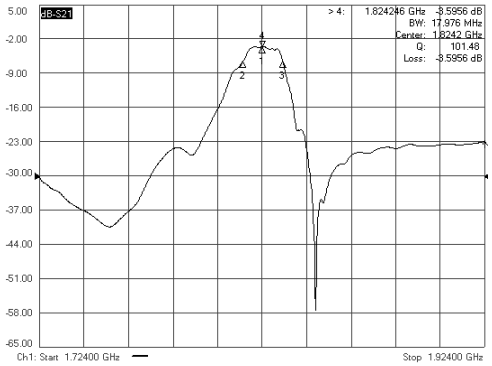

(a)$|S_{21}|$

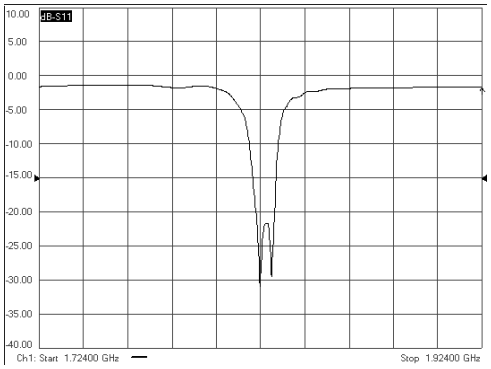

(b)$|S_{11}|$

Figure 5. The measured $|S_{21}|$ and $|S_{11}|$ plots of a TPoS filter (with 50Ω termination).

Bandwidth variation is observed in the IDT structures. An array of filters with similar area of about 120μm×260μm but with different number of fingers are measured, as shown in Fig. 6. It is seen that by increasing the number of fingers (reducing the finger pitch) the frequency spacing between the two coupled modes (BW) is increased. The bandwidth varies from about 4MHz to 25MHz with the total finger number increasing from 9 to 15.

4. ANALYSIS AND DISCUSSIONS

Equivalent circuit model is fitted to the measured results, as shown in Fig. 7. The circuit element values are listed in Table 1, from which the material properties and the possibility for further improvement are investigated.

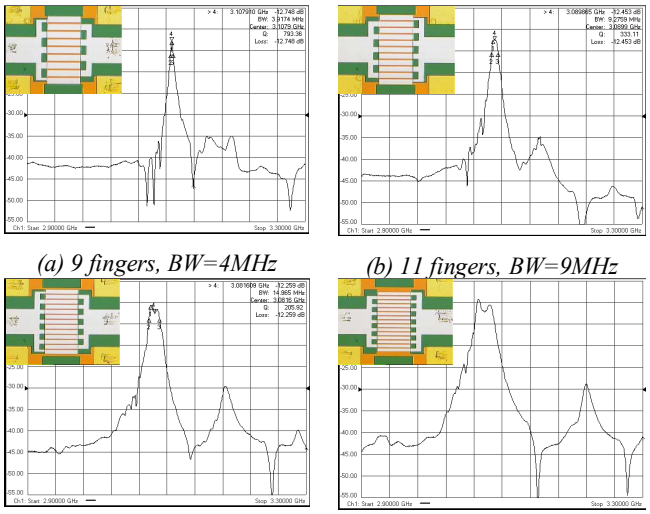

(a) 9 fingers, BW=4MHz *(b) 11 fingers, BW=9MHz*

(c) 13 fingers, BW=15MHz *(d) 15 fingers, BW=25MHz*

Figure 6. Bandwidth tuning measurement of TPoS filters with different finger numbers

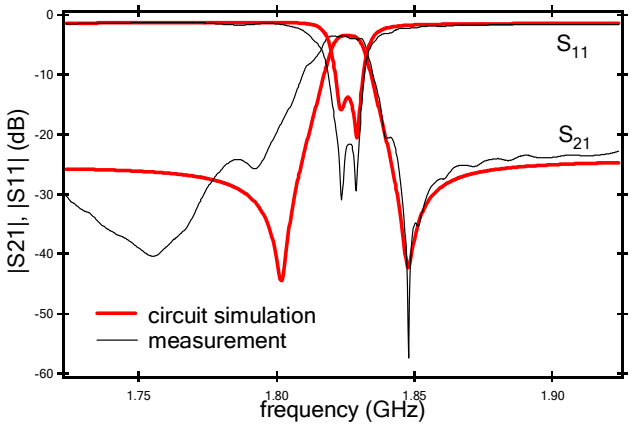

Figure 7. Equivalent circuit simulation fitted to the measurement.

Table 1. Element values of the equivalent circuit.

R_m (Ω)	16		R_p (Ω)	500
L_m (μH)	0.946		L_c (nH)	5
C_m (fF)	8		C_f (fF)	70
C_p (pF)	0.7			

In the series branch, the IL is mainly influenced by the series resistance R_m. The quality factor of the series resonant branch is given by

$$Q_m = \frac{1}{R_m}\sqrt{\frac{L_m}{C_m}} = 680 \qquad (1)$$

implying moderate mechanical damping in the composite structure. Lower IL can be achieved by reducing R_m, realizable by improving the quality of the piezoelectric layer, which both reduces mechanical damping itself and improves the piezoelectric coupling.

In the shunt branch, the IL is mainly influenced by the signal loss through the shunt capacitor C_p and the dissipation

in the shunt resistor R_p. It is seen from the circuit that although the leakage current is eliminated by the introduction of the insulation layer, the shunt resistance R_p is still only 500Ω, implying a large dielectric loss. The relationship between the IL and the shunt resistance R_p is calculated and plotted in Fig. 8 (a). It is seen that the IL can be reduced by increasing the shunt resistance, with IL=2.6dB when R_p=+∞.

The plot also shows that the IL remains almost constant when R_p>1500Ω. In terms of the material's dielectric loss constant (tanδ), approximated by

$$\tan\delta = \frac{1}{\omega C_p R_p}, \qquad (2)$$

at 1.82GHz, R_p=500Ω and 1500Ω correspond to loss tangent of 0.25 and 0.08, respectively. Thus if materials with similar piezoelectric coupling factor but smaller tanδ, such as AlN, is used, the IL of the filter can be further improved.

The relationship between the IL and the shunt capacitance values for different R_p is plotted in Fig. 8 (b). The simulation shows that by reducing the value of C_p, IL can be improved, with the lowest IL when the shunt branch is an open circuit (C_p=0, R_p=+∞). The fully cancellation of C_p can be realized by the implementation of a shunt inductor, which consists of a parallel resonant circuit at the desired frequency.

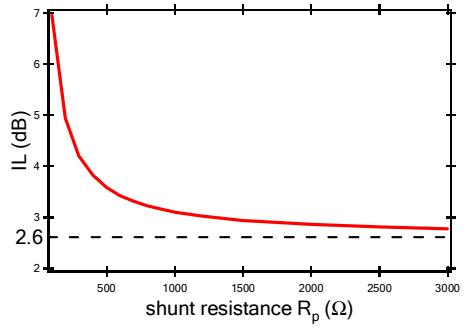

(a) IL vs R_p

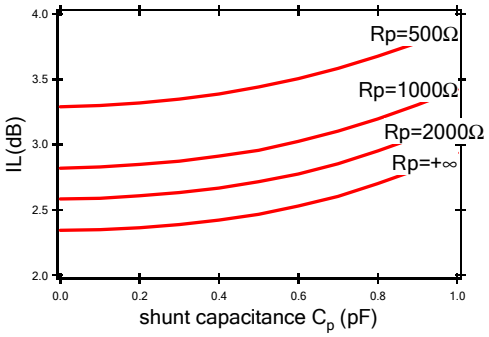

(b) IL vs C_p

Figure 8. The relationship between IL and (a) the shunt resistance R_p, (b) the shunt capacitance C_p.

Assuming the film quality is optimized, for Q_m=*1000* and tanδ=*0.01*, IL of 1.9dB can be achieved, as shown in Fig. 9, comparable to the state-of-the-art ladder-type filters in this frequency range.

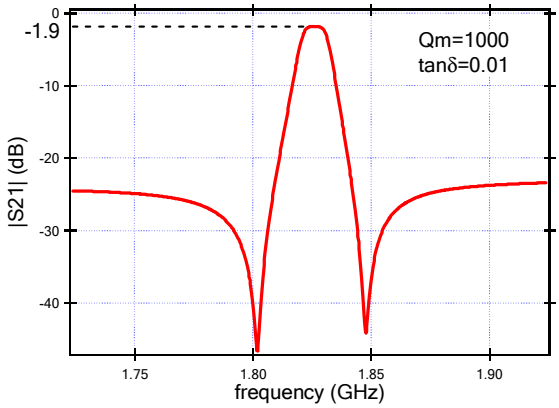

Figure 9. Frequency response of an optimized filter.

5. CONCLUSIONS

We have demonstrated a monolithic thin-film piezoelectric-on-substrate filter with 3.6dB insertion loss and 18MHz bandwidth at 1.8GHz. Such a filter is more compact than commercial ladder-type piezoelectric filters of comparable performance. Analysis of the filter shows that in an optimized situation, IL<2dB can be achieved, making this technology a competitive candidate for modern communication applications.

ACKNOWLEDGMENT

This work is supported by the DARPA Analog Spectral Processor project.

REFERENCES

[1] K. M. Lakin, "Thin Film Resonators and Filters", in *Proc. IEEE Ultrasonics Symposium*, 1999, pp. 895 - 906.

[2] R. Aigner, S. Marksteiner, L. Elbrecht, W. Nessler, "RF-Filters in Mobile Phone Applications", in *Tech. Digest TRANSDUCERS'03 Conference*, 2003, pp. 891 - 894.

[3] R. A. Sykes, W. D. Beaver, "High Frequency Monolithic Crystal Filters with Possible Application to Single Frequency and Single Side Band Use", in *Proc. IEEE Ultrasonics Symposium*, 1966, pp. 288 – 308.

[4] K. M. Lakin, "Coupled Resonator Filters", in *Proc. IEEE Ultrasonics Symposium*, 2002, pp. 901 – 908.

[5] R. Abdolvand, F. Ayazi, "Monolithic Thin-Film Piezoelectric-on-Substrate Filters", in *Tech. Digest IMS'07 Conference*, 2007, pp. 509-512.

[6] L. N. Dworsky, "A Comparison of Band Pass Filter Technologies for Communications System Applications", in *Proc. IEEE Ultrasonics Symposium*, 1991, pp. 241 – 250.

[7] W. P. Mason, "A Dynamic Measurement of the Elastic, Electric and Piezoelectric Constants of Rochelle Salt", *Physical Review*, Vol. 55, pp. 775 – 789, 1939.

[8] J. F. Rosenbaum, *Bulk Acoustic Wave Theory and Devices*, Artech House, Inc., Norwood, MA, 1988.